A fully coherent electron beam from a noble-metal covered W(111) single-atom emitter

Che-Cheng Chang[1,2]**, Hong-Shi Kuo**[1]**, Ing-Shouh Hwang**[1,2,3] **and Tien T Tsong**[1]

[1] Institute of Physics, Academia Sinica, Nankang, Taipei, Taiwan, Republic of China
[2] Department of Materials Science and Engineering, National Tsing Hua University, Hsinchu, Taiwan, Republic of China

E-mail: ishwang@phys.sinica.edu.tw

Abstract
In quantum mechanics, a wavefunction contains two factors: the amplitude and the phase. Only when the probing beam is fully phase coherent, can complete information be retrieved from a particle beam based experiment. Here we use the electron beam field emitted from a noble-metal covered W(111) single-atom tip to image single-walled carbon nanotubes (SWNTs) in an electron point projection microscope (PPM). The interference fringes of an SWNT bundle exhibit a very high contrast and the fringe pattern extends throughout the entire beam width. This indicates good phase correlation at all points transverse to the propagation direction. Application of these sources can significantly improve the performance and expand the capabilities of current electron beam based techniques. New instrumentation based on the full spatial coherence may allow determination of the three-dimensional atomic structures of nonperiodic nanostructures and make many advanced experiments possible.

(Some figures in this article are in colour only in the electronic version)

1. Introduction

The spatial coherence and brightness of electron sources are two key factors for their application to electron interferometry and holography [1–4], electron diffraction [5–7], and electron microscopies [8]. It has been long considered that a smaller source size would yield a higher brightness and a larger transverse coherence width (spatial coherence length or lateral coherence length) [8–10]. Therefore, in principle, single-atom emitters can produce the brightest and most coherent electron beams. Fabrication of single-atom tips for electron sources was first demonstrated by Fink [11, 12]. Subsequently several other methods producing single-atom tips or nanotips were developed [13–15]. Calculations by Scheinfein *et al* suggested that electron beams emitted from tips of atomic size might be totally (or fully) coherent, i.e. the transverse coherence width is equal to or larger than the beam width [10]. Experiments also showed that electron beams emitted from single-atom

emitters or nanotips were significantly more coherent than those from normal tungsten field emitters [16, 17], but full spatial coherence has never been demonstrated. Moreover, those single-atom tips or nanotips have never been put into practical application because they suffer from a short lifetime and their preparation methods are tedious and very unreliable.

A few years ago, Fu *et al* demonstrated that a Pd-covered W(111) single-atom tip could be created through vacuum deposition of one to two monolayers of a Pd film on a clean W tip surface followed by thermal annealing [18]. This tip is basically a nanopyramid grown on top of a larger hemispherical tip. The major advantage of this method is that the growth of a faceted pyramidal tip is a thermodynamic process. Even if the tip is destroyed or contaminated, it can be regenerated through a simple annealing, which ensures its long operation lifetime. Later, this method was modified by Kuo *et al*, with both the preparation of a clean W tip surface and the deposition of a noble-metal film in an electrochemical cell [19]. Pd-, Pt-, Ir-, Rh-, and Au-covered W(111) single-atom tips were successfully produced after the noble-metal plated tips

---

[3] Author to whom any correspondence should be addressed.
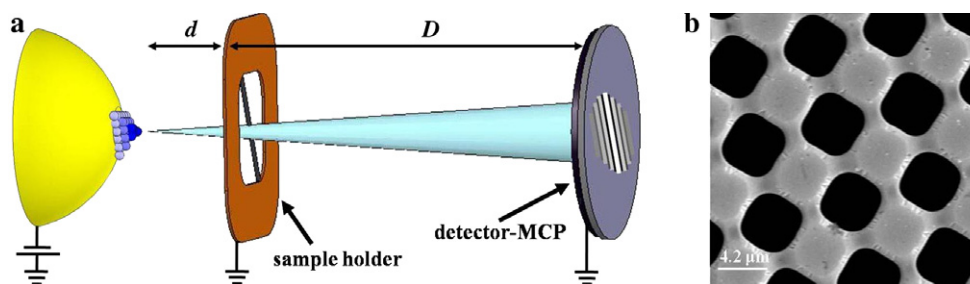
1

Figure 1. Experimental setup. (a) Schematic of the electron point projection microscope. The electron beam is extracted from the topmost atom of the pyramidal single-atom tip. The magnification of the sample at the screen is $(D + d)/d$, where D is 170 mm and d is the tip–sample separation. (b) Scanning electron micrograph of a part of the microfabricated Si_3N_4 membrane. The width of each hole is $\sim$4.2 μm.

were annealed in vacuum [19–21]. These pyramidal tips had the same structure as that of the Pd-covered W(111) single-atom tip prepared by Fu *et al*, and could be regenerated at least several tens of times after destruction by repeated field evaporations. Amazingly, the noble-metal plated tips can be stored in ambient conditions for more than two years before annealing in vacuum. This greatly simplifies the application of these single-atom tips, because annealing is a standard procedure in most instruments that use a field emission tip.

Recent experiments showed that these noble-metal covered W(111) single-atom tips could achieve stable field emission as high as 20 nA [22, 23]. The electron beams have very small opening angles [19–24], which make the brightness of these emitters (reduced brightness of 10^9–10^{11} A m^{-2} sr^{-1} V^{-1}) one to four orders of magnitude higher than those of state-of-the-art electron sources, the Schottky emitter and the normal tungsten field emitter (reduced brightness of $10^7 \sim 10^8$ A m^{-2} sr^{-1} V^{-1}) [8, 25]. It is also better than those of carbon nanotube emitters reported by de Jonge *et al* (reduced brightness of $\sim$$10^9$ A m^{-2} sr^{-1} V^{-1}) [25]. However, no quantitative measurement of the coherence of these single-atom electron sources has ever been reported. This is the main theme of the current work.

The coherence of a source can be evaluated from the interference fringes of nano-objects obtained with a low-energy electron point projection microscope (PPM) [16, 17]. The PPM is a shadow microscope, where an object is placed between a field emission electron point source and a screen. The shadow image of the object can be seen on the screen with a magnification equal to the ratio of the source–screen separation to the source–object separation. If the electron beam is coherent, interference fringes can be seen to be superposed on the shadow image. The contrast and the width of the interference fringes observed at high magnification reveal the spatial coherence of the electron source.

2. Experimental details

Our experiments are carried out with a custom-made electron PPM. Figure 1(a) shows a schematic of the PPM, which is housed in an ultra-high vacuum (UHV) chamber made with mu-metal. Our sample holder is a microfabricated Si_3N_4 membrane coated with a Au film of 50 nm in thickness.

Figure 1(b) shows a scanning electron micrograph of a part of the membrane. The membrane contains periodic holes of width 4.2 μm, which allows suspension of SWNTs across the holes.

The tip used in our experiments is an Ir-covered W(111) single-atom tip. The tip holder is attached to a piezo-scanner that allows fine movements in X–Y–Z directions and the whole assembly is mounted on a stick-slip type linear motor, as in scanning tunneling microscopy, to allow approaching of the tip to the sample. Thus, the tip–sample separation, d, and magnification of the PPM, $M = (D + d)/d$, can be changed. During our experiments, the sample holder is grounded and the tip is negatively biased to extract electrons from the tip end. The projected pattern is recorded with a micro-channel plate (MCP, Hamamatsu F2226-24PGFX, 77 mm in diameter) and a phosphor screen, which are $\sim$170 mm behind the sample. A CCD camera (Alta U2000, 1600 pixels $\times$ 1200 pixels, 16-bit dynamic range) is placed behind the screen to take images. For all the results presented in this work the tip is kept at room temperature during electron emission.

To prepare an Ir/W(111) single-atom tip, a single crystal W(111) wire of 0.1 mm in diameter is first etched to a sharp tip in a KOH solution, followed by cathodic cleaning and electroplating of a thin Ir film on the tip end. A conventional 3-electrode electrochemical cell is used which has a Pt counter electrode and a saturated calomel reference electrode (SCE). The W tip is placed at the working electrode. To decrease the area for metal deposition, we use nail polish to shield the tip from the electrolyte except for the apex. After that, the tip is immersed into 0.1 M HCl of 20 ml and held at -0.6 V (SCE) to reduce the surface oxide for about 3 min. Then, a small amount of plating electrolyte (0.1 mM $IrCl_2$, 15 μl) is dropped into the electrochemical cell under the same cathodic polarization. The Faradic current is monitored during the electrochemical process, and the deposition time is $\sim$5 s. Before the vacuum process, acetone is used to remove the nail polish on the tip [19–21]. The plated tip is mounted onto a tip holder of the PPM. Under the UHV condition, the plated tip is annealed through e-beam bombardment by applying $+500$ V to the tip for $\sim$5 min. The e-beam is emitted from a heated tungsten coil placed near the tip.
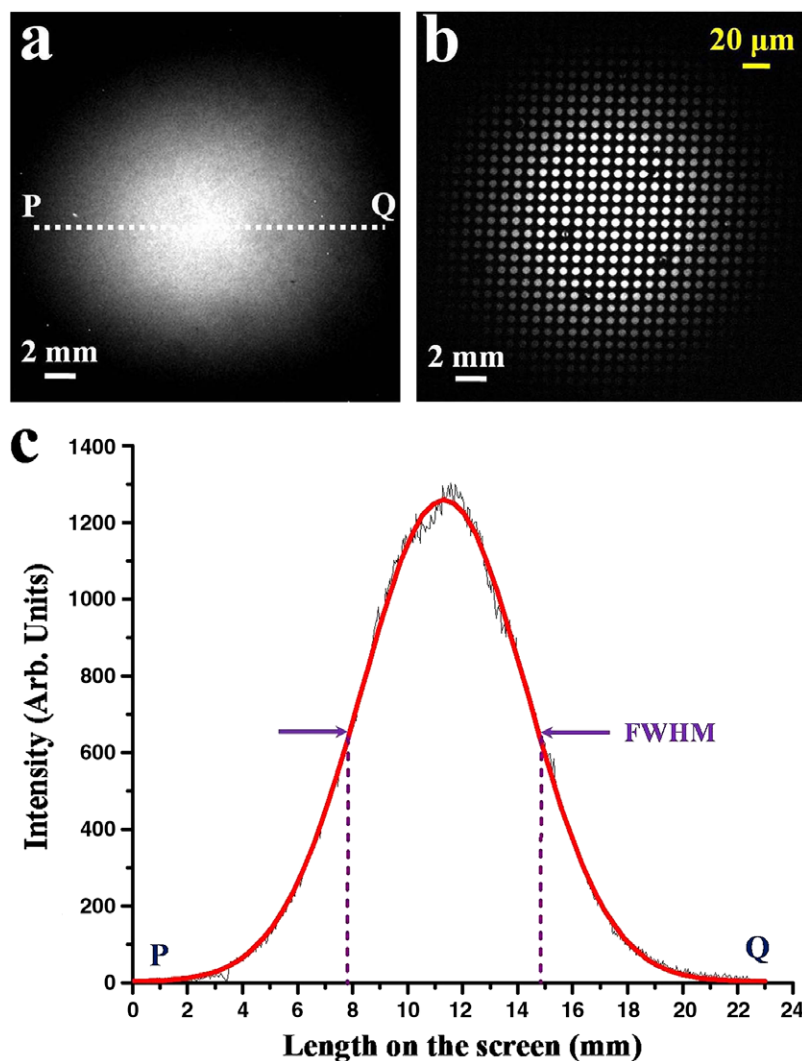
Figure 2. Electron beam profile. (a) Field emission pattern of the single-atom tip. The emission current is ∼40 pA. The scale bar at the lower left-hand corner indicates a length of 2 mm on the screen, corresponding to an angle of 0.67°. (b) Point projection image of our sample holder when $d = 4$ mm. The tip bias is −500 V. The yellow scale bar at the upper right-hand corner indicates a length of 20 μm on the sample plane. (c) Intensity profile of the field emission pattern along the dotted line PQ in (a) with fitting of a Gaussian distribution (the thick red curve).

3. Results and discussion

3.1. Narrow Gaussian beam

Figure 2(a) is a field emission pattern taken with a single-atom tip at a voltage of −1400 V. The sample holder is removed in this case. The pattern exhibits a round spot and the line profile of the intensity can be well fitted with a Gaussian distribution having standard deviation $\sigma = 4.5$ mm, as shown in figure 2(c). The beam diameter is often defined as the full width half maximum (FWHM), which is measured to be ∼7 mm, corresponding to an opening angle (2θ) of only 2.4°. This value is similar to those obtained by Oshima *et al* on several noble-metal covered W(111) single-atom tips [22–24] and significantly smaller than those reported by Kuo *et al* [19–21]. The projection image through the sample holder also exhibits a similar narrow beam profile, as seen in figure 2(b), when the tip is 4 mm away from the sample. In figure 2(b), the regularly spaced bright spots corresponding to the holes in the

Si_3N_4 membrane indicate that little distortion is caused by our PPM and CCD camera. The spacing between the holes and the size of the holes can also be used for length calibration in PPM images.

For noble-metal covered W(111) single-atom tips, the relationship between the field ion microscopy (FIM) image and the corresponding electron field emission pattern have been well studied [19–21, 23, 24]. From our experiments on several single-atom tips, the round emission spot with a FWHM of 6–9 mm, corresponding to an opening angle of 2°–3° as in figure 2(b), indicates the formation of a single-atom tip.

3.2. Full spatial coherence

When the tip is moved closer to the sample, the projection image shows a higher magnification of the sample, which is inversely proportional to the tip–sample separation, d. Figure 3(a) shows a projection image of several interconnected SWNT bundles inside a hole taken at a tip voltage of −150 V.
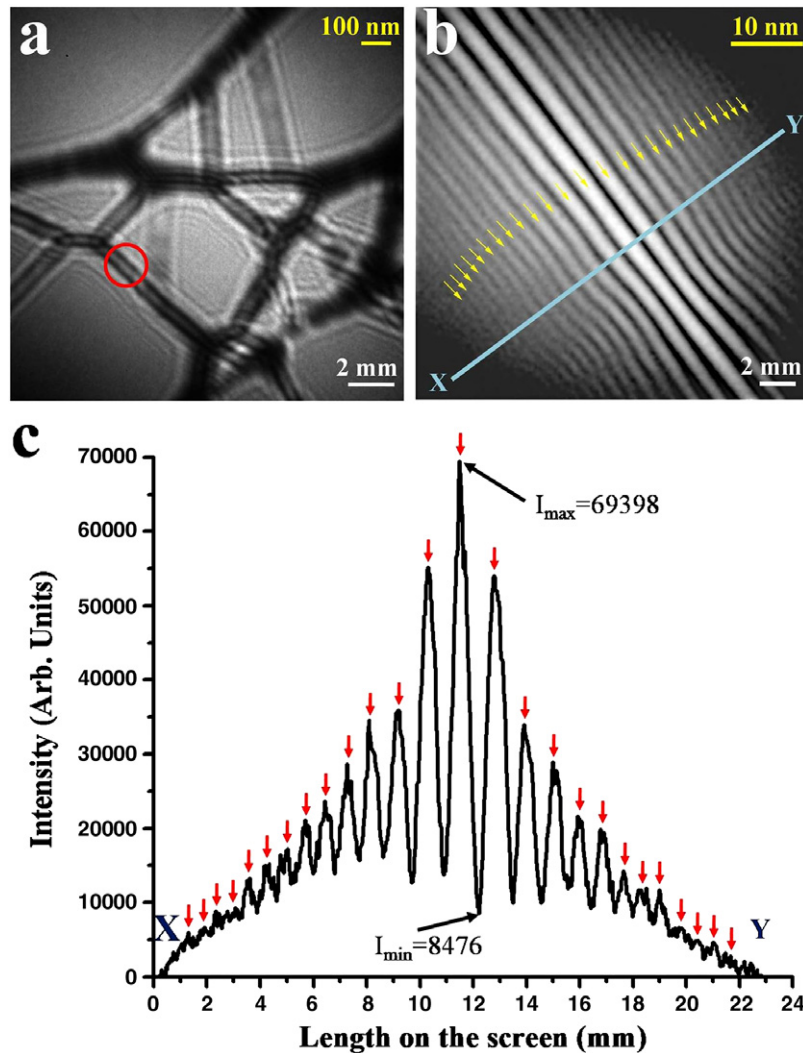
Figure 3. Interference patterns of SWNT bundles. (a) Point projection image of several interconnected SWNT bundles with $d = 12$ μm. The tip bias is -150 V. (b) Point projection image of a SWNT bundle with $d = 425$ nm. The tip bias is -89 V. The emission current is $\sim$0.5 nA. Each fringe is indicated with an arrow. In (a) and (b), the scale bar at the lower right-hand corner indicates a length of 2 mm on the screen; the yellow scale bar at the upper right-hand corner indicates a length as indicated on the sample plane. (c) Intensity profile along the line XY in (b). Each fringe is indicated with an arrow. Background signals, which are taken when the electron emission is turned off, have been subtracted pixel-by-pixel from the measured signals.

Interference fringes around these bundles are clearly seen. These interference fringes are similar to PPM images of carbon fibers reported previously [16, 17]. Figure 3(b) shows an image taken at a tip voltage of -89 V after a further approach toward the SWNT bundle indicated with a circle in figure 3(a). Amazingly, the fringe pattern now spans the entire bright area on the screen. More than 25 fringes are visible.

An intensity profile XY across the fringe pattern is shown in figure 3(c). The oscillation in intensity can be seen throughout the entire beam with detectable intensity, indicating good phase correlation in the plane perpendicular to the beam axis. This intensity profile also suggests that the transverse coherence width could be equal to or larger than $\sim$20 mm, which is significantly larger than twice the FWHM of the electron beam. The interference pattern in figure 3(b) can be roughly understood in the following way. The SWNT bundle can act as a nanoprism in a PPM [26]. The nanoprism splits

the wavefront of an incoming electron wave into two coherent partial waves, which are deflected by the electric fields around the nanoprism in opposite directions and meet on the screen. Under normal action of a biprism, the fringes in the overlap region of the two waves are regularly spaced. The center three bright fringes in figure 3(b) exhibit the same spacing and very high contrast, suggesting that the central part of the beam is strongly phase correlated. The other fringes outside the center three may mainly result from the Fresnel edge interference, suggesting good phase correlation between the center and the edge of the beam. This can basically explain the full spatial coherence of the electron beam.

A common method to quantify the degree of coherence is the measurement of visibility from the interference fringes, where visibility $V = (I_{max} - I_{min})/(I_{max} + I_{min})$ [3, 4, 8]. The more coherent the beam is, the larger V can be obtained, which means a better contrast of the fringes. We obtain a value

of 0.78 for the visibility, with I_{max} taken as the maximum value of the highest peak and I_{min} as the minimum value of the valley next to it. This value is higher than those (0.6–0.7) reported recently with a coherent source from a tungsten field emitter at 77 K [26], and far exceeds the values obtained with other sources. We note that the visibility value higher than 0.7 can be consistently obtained with this type of single-atom tip.

In the ideal case of interference from monochromatic plane waves with uniform intensity in the lateral directions, V can reach a maximum value of 1. The reason our visibility is lower than 1 may come from several factors. One factor is the energy spread of our electron source, 0.3–0.4 eV [23, 24, 27], which is slightly higher than that of a tungsten field emitter, 0.3 eV. Another factor may come from the contribution of inelastic scattering by the SWNT bundle of 10 nm in diameter, which is much larger than the inelastic mean free path (0.5–1.0 nm) for low-energy electrons of ~100 eV [28]. Furthermore, the visibility value should be reduced by a certain degree for the very narrow Gaussian beam, in which the intensity decays rapidly away from the center.

3.3. Spatial coherence of sources of atomic size

Another measure of spatial coherence is the ratio K ($=\xi_T/\sigma$) proposed by Pozzi [29], where ξ_T is the transverse coherence width of the electron beam. Pozzi has proved that K remains a constant at all positions of electron optics, and he considered $K \gg 1$ ($K \ll 1$) for a coherent (incoherent) beam. Here we would like to define total coherence for the case of $K \geqq 2$.

Traditionally, using the van Cittert–Zernike (VCZ) theorem, ξ_T can be estimated from the effective source size (radius), r_i, through the relation $\xi_T = \lambda D/\pi r_i$, where λ is the electron wavelength [10, 29]. In general, r_i is smaller than or equal to the real geometrical size [26]. However, for a source as small as a single atom, one also needs to consider the limitation set by Heisenberg's uncertainty principle, $\Delta x \cdot \Delta p_x \geqslant h/4\pi$, where h is Planck's constant. Δx is the uncertainty in position, so $\Delta x \sim r_i$. Δp_x is the uncertainty in momentum, and $\Delta p_x = p \sin(\theta_{rms}) \sim (h/\lambda)\theta_{rms}$, where $\theta_{rms} = \sigma/D$ is the half opening angle of the beam measured in terms of standard deviation. From the uncertainty principle, we derive $r_i \geqslant \lambda/(4\pi\theta_{rms})$. We can set $r_i \sim \lambda/(4\pi\theta_{rms})$, which is the smallest source size we can discern if the real source size is smaller than this value. Thus, we obtain $\xi_T \sim 4D \cdot \theta_{rms} = 4\sigma$ and the ratio $K \sim 4$ for a single-atom source. With an electron beam of 89 eV as in figure 3(b), corresponding to the electron wavelength of 1.30 Å, we obtain $r_i \sim \lambda/(4\pi\theta_{rms}) \sim 3.9$ Å. This effective source size is larger than the real size of a single-atom tip (1–2 Å). The values of $\xi_T \sim 4\sigma$ and $K \sim 4$ are consistent with our observation of interference fringes shown in figure 3(b).

However, the VCZ theorem has an assumption: the effective source is a collection of mutually uncorrelated emission points. This theorem provides a good estimation for the coherence width of a broad source, such as a normal tungsten field emitter, but may well underestimate that of a source of atomic size, such as a single-atom tip, a trimer tip, or any source <1 nm. Pozzi also pointed out that the electron beam would be fully coherent under the condition of a coherent source, i.e. $r_i \ll R_A$, where $R_A = \lambda/(\pi\theta_{rms})$ can be viewed as the coherence width at the effective source due to the angular divergence of the beam [29]. For an electron beam of 89 eV emitted by our single-atom tip, R_A is estimated to be 15.6 Å when $\theta_{rms} = 1.7°$, much larger than the real source size and the effective source size estimated above. This indicates that the values of $\xi_T \sim 4\sigma$ and $K \sim 4$ for our electron source obtained with the VCZ theorem above may well be underestimated. New theoretical and experimental methods are needed to address the transverse coherence width for a source of atomic size.

3.4. Applications of noble-metal covered W(111) single-atom tips

In electron holography, the phase images allow quantitative determination of electric and magnetic fields in a material down to atomic dimension [3, 4]. In coherent electron diffraction, methods have been developed to determine the three-dimensional atomic-resolution image of nonperiodic nanostructures [5–7]. In general, the more coherent the beam is, the better the quality of the high-resolution phase contrast images, the sharper the diffraction patterns, and the better the diffraction contrast. Both the brightness and spatial coherency of noble-metal covered W(111) single-atom sources are orders of magnitude better than those of normal tungsten field emitters. Utilization of these fully coherent single-atom sources would significantly improve the performance of electron holography and coherent electron diffraction. This would have great impact on materials science and technology.

The very small opening angles of noble-metal covered W(111) single-atom sources provide additional benefits. It allows the operation of electron microscopes with good brightness even at low voltages because of very small spherical aberration. Low brightness at low voltages is a major limitation of current electron microscopes. Operation at a lower voltage would have higher image contrast for light elements, such as carbon, oxygen, and nitrogen, which are major elements in biological specimens. Development of low-voltage electron microscopes would broaden the applications of electron microscopies. In addition, many new electron beam based instruments may be developed based on this type of high-performance electron source.

Here we would also like to propose a new coherent electron diffraction scheme based on the PPM scheme shown in figure 1(a). With $d = 1$ μm, the FWHM of the electron beam from a noble-metal covered W(111) single-atom tip is only ~40 nm on the sample plane. This allows the coherent diffractive imaging of an isolated object of 40 nm or smaller. Only the MCP and screen should be moved very close to the sample to record the diffraction pattern at large angles. This PPM based scheme would be much simpler and more economical than current TEM based coherent electron diffraction [6]. It is especially suitable for imaging small biological molecules, because the scattering cross sections of light elements are very large and radiation damage is almost negligible for the low-energy electrons.

5

4. Conclusions

We have demonstrated full spatial coherence of an electron beam emitted from a noble-metal covered W(111) single-atom tip. The total coherence and very high brightness of this type of single-atom source can significantly improve the performance and expand the capabilities of current electron microscopies, electron interferometry and holography, and electron diffraction. We anticipate that the fully coherent electron beam will also make possible many advanced electron beam based experiments.

Acknowledgments

References

[1] Gabor D 1948 *Nature* **161** 777
[2] Missiroli G F, Pozzi G and Valdrè U 1981 *J. Phys. E: Sci. Instrum.* **14** 649
[3] Tonomura A 1987 *Rev. Mod. Phys.* **59** 639
[4] Liche H and Lehmann M 2008 *Rep. Prog. Phys.* **71** 016102
[5] Miao J, Ohsuna T, Hodgson K O and O'Keefe A 2002 *Phys. Rev. Lett.* **89** 155502
[6] Zuo J M, Vartanyants I, Gao M, Zhang R and Nagahara L A 2003 *Science* **300** 1419
[7] Zuo J M, Gao M, Tao J, Li B Q, Twesten R and Petrov I 2004 *Microsc. Res. Tech.* **64** 347
[8] Williams D B and Carter C B 1996 *Transmission Electron Microscopy* (New York: Plenum)
[9] García N and Rohrer H 1989 *J. Phys.: Condens. Matter* **1** 3737
[10] Scheinfein M R, Qian W and Spence J C H 1993 *J. Appl. Phys.* **73** 2057
[11] Fink H W 1986 *IBM. J. Res. Dev.* **30** 460
[12] Fink H W 1988 *Phys. Scr.* **38** 260
[13] Janssen A P and Jones J P 1971 *J. Phys. D: Appl. Phys.* **4** 118
[14] Binh V T and Garcia N 1992 *Ultramicroscopy* **42** 80
[15] Nagaoka K *et al* 2001 *Appl. Surf. Sci.* **182** 12
[16] Fink H W, Stocker W and Schmid H 1990 *Phys. Rev. Lett.* **65** 1204
[17] Binh V T, Semet V and Garcia N 1994 *Appl. Phys. Lett.* **65** 2493
[18] Fu T Y, Cheng L C, Nien C H and Tsong T T 2001 *Phys. Rev.* B **64** 113401
[19] Kuo H S *et al* 2004 *Nano Lett.* **4** 2379
[20] Kuo H S *et al* 2006 *e-J. Surf. Sci. Nanotechnol.* **4** 233
[21] Kuo H S *et al* 2006 *Japan. J. Appl. Phys.* **45** 8972
[22] Ishikawa T *et al* 2007 *Appl. Phys. Lett.* **90** 143120
[23] Oshima C *et al* 2005 *e-J. Surf. Sci. Nanotechnol.* **3** 412
[24] Itagaki T *et al* 2007 *Surf. Interface Anal.* **39** 299
[25] de Jonge N, Lamy Y, Schoots K and OOsterkamp T H 2002 *Nature* **420** 393
[26] Cho B, Ichimura T, Shimizu R and Oshima C 2004 *Phys. Rev. Lett.* **92** 246103
[27] Rokuta E *et al* 2008 *Surf. Sci.* **602** 2508
[28] Zangwill A 1988 *Physics at Surfaces* (Cambridge: Cambridge University Press)
[29] Pozzi G 1987 *Optik* **77** 69